Detecting cerebral palsy in neonatal stroke children: GNN-based detection considering the structural organization of basal ganglia

Patty Coupeau, Jean-Baptiste Fasquel, Josselin Démas, Lucie Hertz-Pannier, Mickael Dinomais

DETECTING CEREBRAL PALSY IN NEONATAL STROKE CHILDREN: GNN-BASED DETECTION CONSIDERING THE STRUCTURAL ORGANIZATION OF BASAL GANGLIA

Patty Coupeau [1⋆], *Jean-Baptiste Fasquel* [1], *Josselin Demas* [1,2], *Lucie Hertz-Pannier* [3], *Mickaël Dinomais*[1,4]

[1] Universite d'Angers, LARIS, SFR MATHSTIC, F-49000 Angers, France
[2] Instituts de Formation, CH Laval, France
[3] UNIACT/Neurospin/JOLIOT/DRF/CEA-Saclay, and U1141 NeuroDiderot/Inserm, CEA, Paris University, France
[4] Department of Physical and Rehabilitation Medicine, University Hospital, CHU Angers, France

ABSTRACT

As a long-term consequence of neonatal arterial ischaemic stroke (NAIS), the presence of cerebral palsy (CP) depends on the structural integrity of brain areas, especially of basal ganglia. Yet, it remains challenging to establish an early diagnosis of CP from a conventional structural MRI. In this study, we introduce a graph neural network-based classification for the recognition of NAIS children and mainly for the detection of children with CP among the NAIS ones. From the structural MRI of 68 children aged 7 years old and their corresponding segmentation of basal ganglia, we construct graphs where nodes represent structures, carrying on node and edge attributes structural information (volumes, distances). The classification accuracy achieved by the proposed method is of 86% for the detection of NAIS and of 89% for the detection of CP among neonatal stroke children.

***Index Terms*—** Cerebral palsy, neonatal arterial ischaemic stroke, basal ganglia structural organization, graph neural network, graph classification

1. INTRODUCTION

With a birth prevalence of 1/4000, neonatal arterial ischaemic stroke (NAIS) is the most common and frequent of childhood stroke [1]. NAIS is defined as a cerebro-vascular event occurring between birth and 28 postnatal days with evidence of focal arterial infarction [2]. Around 20-30% of term infants with NAIS will develop unilateral cerebral palsy (CP) which is the most frequent motor impairment in children [2]. As a rule, infants with the most extensive brain lesions are at highest risk for long-term disabilities [3]. However, some infants in whom brain lesions are relatively small but specifically located along the motor pathway in the cerebrum may also develop CP [4]. Apart from the most severe cases, the motor outcome is difficult to predict from neonatal conventional MRI. Prediction of the motor developmental trajectory remains challenging and new clinical and/or radiological tools are under development to better predict long-term motor outcome [5]. Establishing an early diagnosis of CP and understanding the occurrence of CP are important as this can expedite motor rehabilitation intervention. In previous work [6], we demonstrate that, as a long-term consequence of NAIS, presence or absence of CP depends on the structural integrity of brain areas anatomically remote from the infarct site (ispilesional thalamus). Broadly, the basal ganglia appears as a major component of preserving motor function following early brain lesion [7].

⋆Corresponding author: patty.coupeau@univ-angers.fr

Thus, we present a method of diagnosing CP from a structural MRI not only based on volume relations as in [7] but also on the spatial organization of the basal ganglia. For that, we propose to work with graphs where each node represents a brain structure extracted from the MRI and the edges carry the distance between structures. The detection of CP is then done using a graph neural network (GNN) [8] trained to perform binary classification. Working with graphs allows to represent more explicitly spatial relationships between structures than machine learning classifiers where volumes and distances would be covariates. The use of graphs to diagnose pathology from MRI has recently been proven (neuropsychiatric disorders classification [9], graph-based diagnosis of autism spectrum disorder [10]). Our proposal has the advantage of working with small graphs (only 8 nodes) and simple attributes (volumes, distances), thus requiring fewer training parameters than a direct CNN-based classification from the image. Our main contribution lies in the original proposed GNN-based method to recognize children with NAIS but also to diagnose the presence of CP among these children from a structural T1-weighted MRI.

The proposal is described in Section 2. Experiments are detailed in Section 3 and discussed in Section 4.

2. METHOD

Figure 1 provides an overview of the proposed approach. From the segmentation of basal ganglia on MRI, we construct a graph where only symmetrical structures are linked. Beforehand, from the segmentation of control subjects, we build the matrix D_{ref} of the average distance between the barycenters of each brain structure, being required to compute edge attributes of graphs for both training (A) and inference (B). A GNN (C) is then trained with these graphs to predict the class y of the subject.

2.1. Graph construction

We define the graph $G = (V, E, X, L)$ where V is the set of nodes (each node $v \in V$ corresponds to a basal ganglia structure) and E is the set of edges. We propose to connect only the supposedly symmetrical structures (i.e. left caudate with right caudate, etc.) since we want to highlight an asymmetry between hemispheres. X is a node attribute assignment function $X : V \to \mathbb{R}$ regarding the volume of the corresponding structure normalized to the total brain volume. L is an edge attribute assignment function $L : E \to \mathbb{R}$ such as:

$$L(i,j) = \frac{1}{3}\sum_{k=1}^{3} 1 + |1 - \frac{d_k^{i,j}}{D_{\text{ref},k}^{i,j}}| \quad (1)$$

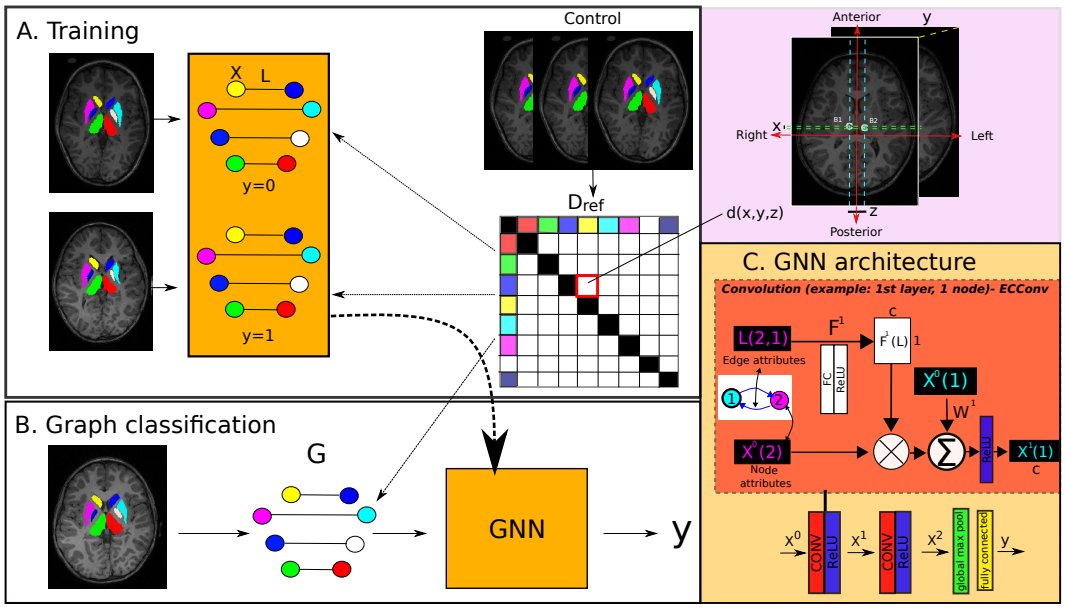

Fig. 1. Overview of the proposed GNN-based method for NAIS and PC detection

where $d_k^{i,j}$ indicates the distance between nodes i and j in the direction k and $D_{\text{ref},k}^{i,j}$ indicates the average distance between structures i and j in the direction k for control children. D_{ref} is previously constructed, from the MRI of control subjects, as the average on all these children of the distance between the barycenters of every segmented structures (basal ganglia) according to the 3 axes (x: anterior-posterior, y: inferior-superior and z: right-left). Thus, in Figure 1, the red box in D_{ref} indicates the control average distance between the right and left caudate along the 3 axes. The edge attributes are computed to be greater than 1 in order to avoid too small values (close to 0) which would cancel the node attributes during the convolution operation described in Eq.2 (hereafter detailed).

2.2. Graph neural network

As illustrated in Figure 1-C, the architecture of the proposed GNN is composed of 2 graph convolution layers (with output channel dimensions c being an hyperparameter except for the 2$^{\text{nd}}$ layer where $c = 2$ in this work) followed by affine ReLU activation, a global max pooling and a fully-connected layer with two output channels corresponding to the two classes. The aggregation of the neighborhood information takes place within the convolution operations. We consider the graph convolution operator ECConv [11] due to its ability to manage scalar but also multi-dimensional edge attributes. Note that, we could have considered other convolution operators managing edge attributes such as GATConv [12]. Let $X^l(i)$ be the attribute of node i at layer $l \in [1, 2]$ and $L(i, j)$ the scalar attribute of the edge connecting nodes i and j. The message passing at layer l can be defined as [11]:

$$X^{l+1}(i) = \sigma(W^{l+1}X^l(i) + \sum_{j \in N(i)} F^{l+1}(L(j,i))X^l(j)) \quad (2)$$

where σ denotes the ReLU function, $W^{l+1} \in \Re^{c \times 1}$ is a matrix of trainable weights and $F^{l+1} : \Re \rightarrow \Re^{c \times 1}$ is a differentiable function (a multi-layer perceptron). $N(i)$ represents all nodes j neighboring i (connected to i). Then, the global max pool operator returns a graph-level output by taking the channel-wise maximum across the node dimension, so that its output is computed by: $y_g = \max_{i \in V} X^2(i)$. y_g (2-dimensional vector) then passes through a linear layer (FC) whose output $\hat{y}$ is of dimension 2. The class y of the graph is computed as the argmax of $\hat{y}$.

3. EXPERIMENTS

We divide the experiments into two parts. First, we perform a binary classification to recognize children with NAIS among healthy controls. This task is considered to evaluate whether the proposal is able to distinguish two visually distinct populations. Then, we present a classification to detect children with CP among children with NAIS.

3.1. Dataset

Our method is evaluated with a cohort of 68 children aged 7 years old. These children include healthy controls and children with injury in the right or left hemisphere. Each child got an MRI scan (3D T1-weighted volumes of 256x256x176 voxels with a spatial resolution of 1x1x1mm^3). A first atlas-based segmentation is performed using the Hammersmith atlas [13]. Then, each MRI is manually corrected slice by slice with ITKSnap [14]. Each segmentation is visually checked and validated by consensus with a specialist.

Concerning the detection of children with cerebral palsy, we kept in our dataset only the 37 children with NAIS. All children were examined during the 7-year assessment by an experienced clinician (paediatric neurologist, paediatric rehabilitation specialist). The definition of cerebral palsy provided by the Surveillance of CP in Europe Network (SCPE) [15] was used. Among the 37 children, 13 children were diagnosed as having CP.

3.2. Evaluation protocol

All the experiments are carried out in a Python environment using the PyTorch Geometric library [16]. The GNN architecture pre-

sented in Section 2.2 is used by setting the output dimension c of the first convolution layer to 5. The model is trained with Adam (Adaptive Moment Estimation), on 300 epochs with a learning rate $l_r = 0.001$. A binary cross-entropy loss function is considered. Distribution of the dataset for both experiments in training and test data is presented in Table 1. A cross-validation strategy is implemented to test our method on all the children while having sufficient training data. To deal with the imbalanced dataset (e.g. only 13 children with CP vs 24 without), 3 stratified random samplings (all with the distribution indicated in Table 1) are conducted in both cases (results are averaged over the 3 draws). Twenty training control subjects are used to compute the reference distances (D_{ref} in Figure 1).

	Train		Test	
NAIS detection	Control	NAIS	Control	NAIS
Distribution	20	25	11	12
CP detection	No CP	CP	No CP	CP
Distribution	16	9	8	4

Table 1. Training and test dataset sizes for both experiments i.e. detection of neonatal stroke (NAIS) and of cerebral palsy (CP). 3 stratified draws with the indicated distribution are considered in both cases.

To assess the performance of the method, we measure the balanced accuracy of classification [17]. We also study the complementarity of both node and edge attributes.

3.3. Results

	No attr.	Edges	Nodes	Nodes+Edges
NAIS	0.5	0.63	0.82	**0.86**
PC	0.5	0.67	0.85	**0.89**

Table 2. Complementarity of node and edge attributes for NAIS and PC detection (in terms of balanced accuracy). no attr: no attributes.

3.3.1. Recognition of neonatal stroke children

Table 2 (1st line) reports the classification performances obtained. We observe that our method reaches an accuracy of 86%.

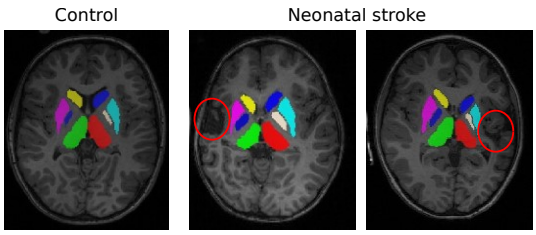

Fig. 2. NAIS detection: example of MRI of both classes. Left: control brain with a good symmetry between hemispheres. Right: injured brains (the lesion is circled in red).

This is a simple task since the difference between the two classes can be done visually with an MRI by detecting the lesion and evaluating the symmetry between each hemisphere (Figure 2). Nevertheless, it validates the ability of the method to classify populations based on the structural information of basal ganglia. It also demonstrates the complementarity of each attribute. Indeed, in Table 2, we observe that the node attributes increase the balanced accuracy from 0.5 to 0.82. Even if the combination of both attributes little improves the results (0.82 to 0.86), we observe that edge attributes help for the classification (balanced accuracy of 0.63 vs 0.5 without any attribute).

3.3.2. Detection of cerebral palsy among children with NAIS

Table 2 (2nd line) reports the classification performances obtained. Proposal reaches an accuracy of 89% on the 37 children. Details of the classification are shown in Table 3.

Truth \ Predicted	No CP	CP
No CP	**22**	2
CP	2	**11**

Table 3. Confusion matrix for the classification of NAIS children with and without cerebral palsy.

Of the 24 children without CP, 22 are correctly classified. In the same way, our method allows to detect 11 children with CP over the 13 in the cohort. In total, the proposal is wrong on 4 children which is a rather good result considering the difficulty of the problem mentioned previously and illustrated in Figure 3. Indeed, it is difficult to distinguish the populations since both have a lesion. The proximity of the lesion to the basal ganglia plays a role but it is visually difficult to make a decision (i.e. does the child has a PC?).

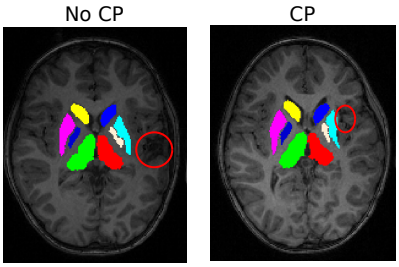

Fig. 3. PC detection: Example of MRI of both classes. Left: injured brain without cerebral palsy. Right: injured brain of a child with cerebral palsy. Lesion is circled in red.

We observe the complementarity of node and edge attributes, each improving the accuracy in the classification task (Table 2).

4. DISCUSSION

This work illustrates a relationship between the structural organization of basal ganglia and the motor function of children. The combination of the structure volumes and of the distances between "symmetrical" structures in a graph allows to recognize children with neonatal stroke with a balanced accuracy of 86% but also to recognize in most cases (89%) children with NAIS who have developed cerebral palsy. Classification of the subjects is done through a GNN with a small architecture (79 trainable parameters). These good performances need to be compared to competing methods for classification problems like non-graph machine learning classifiers (e.g. SVM, TabFPN [18]) or deep learning methods operating directly from the image (CNN-based classification) to confirm the relevance of such a simple graph-based method. Results are obtained

with a dataset size similar to those considered for such studies: 40 children in *Lee et al* [3], 64 children in *Hassett et al* [7] including 20 controls and 44 with neonatal stroke while we consider 68 children including 31 controls and 37 with NAIS. However, they need to be confirmed on other populations. Indeed, the study is performed on 7-year-old children but we should wonder if the relationship between structures and motor functions remains true at other ages, especially to diagnose CP in the early years of the child. A deepening of this work would be to study a possible correlation between structural organization of the basal ganglia and clinical scores describing children's motor skills. This regression problem might require more attributes on nodes and edges but also other modality of MRI like functional MRI as proposed by [10]. Such a prompt detection of motor deficit after NAIS appears necessary to implement early motor interventions.

The method lies in the need of a segmentation of the basal ganglia. However, in the case of stroke brains, this is a complex operation [7], not yet automated, and thus operator-dependent. To make our method really efficient, it would be necessary to automate this preliminary step of basal ganglia segmentation.

5. CONCLUSION

We propose a GNN-based strategy to detect cerebral palsy in neonatal stroke children considering the structural organization of the basal ganglia (volumes, distances between structures), this having never been studied yet. Perspectives for this work are numerous. We aim to study a possible correlation between the structural organization of the basal ganglia and various clinical scores in order to detect a motor deficit after NAIS from an MRI. This would help to set up early motor interventions. Furthermore, we will apply the method to younger children to attempt to diagnose CP early in children with NAIS. This could also be applied to children who have begun rehabilitation in order to evaluate the effectiveness of care. Finally, we will reinforce the efficiency and robustness of the method by automating the segmentation of basal ganglia on injured brains and by comparing the use of other graph convolution operators in the GNN.

6. COMPLIANCE WITH ETHICAL STANDARDS

The AVCnn study (PHRC regional n°0308052 and PHRC interrégional n°1008026; eudract number 2010-A00329-30; Clinical trial NCT02511249) was done in accordance with the international ethical standards and the Declaration of Helsinki. The current evaluation at 7 years was approved by the regional ethics committee (Comité de protection des personnes Sud-Est 1) on May 25^{th} 2010. Informed consent was obtained from each participant.

7. ACKNOWLEDGMENTS

No funding was received for conducting this study. The authors have no relevant financial or non-financial interests to disclose.

8. REFERENCES

[1] A. Kirton and G. deVeber, "Paediatric stroke: pressing issues and promising directions," *Lancet Neurology*, vol. 14, pp. 92–102, 2015.

[2] S. Chabrier, B. Husson, M. Dinomais, et al., "New insights (and new interrogations) in perinatal arterial ischemic stroke," *Thrombosis Research*, vol. 127, pp. 13–22, 2011.

[3] J. Lee, L. A. Croen, C. Lindan, et al., "Predictors of outcome in perinatal arterial stroke: a population-based study," *Annals of Neurology*, vol. 58, pp. 303–308, 2005.

[4] M. Dinomais, L. Hertz-Pannier, S. Groeschel, et al., "Long term motor function after neonatal stroke: lesion localization above all," *Human Brain Mapping*, vol. 36, pp. 4793–4807, 2015.

[5] B. Husson, L. Hertz-Pannier, C. Renaud, et al., "Motor outcomes after neonatal arterial ischemic stroke related to early MRI data in a prospective study," *Pediatrics*, vol. 126, pp. 912–918, 2010.

[6] S. Chabrier, E. Peyric, L. Drutel, et al., "Multimodal outcome at 7 years of age after neonatal arterial ischemic stroke," *The Journal of Pediatrics*, vol. 172, pp. 156–161, 2016.

[7] J. Hassett, H. Carlson, A. Babwani, and A. Kirton, "Bihemispheric developmental alterations in basal ganglia volumes following unilateral perinatal stroke," *NeuroImage: Clinical*, vol. 35, 2022.

[8] D. Bacciu, F. Errica, A. Micheli, and M. Podda, "A gentle introduction to deep learning for graphs," *Neural Networks*, vol. 129, pp. 203–221, 2020.

[9] L. Liu, Y.-P. Wang, Y. Wang, et al., "An enhanced multimodal brain graph network for classifying neuropsychiatric disorders," *Medical Image Analysis*, vol. 81, 2022.

[10] W. Yang, G. Wen, P. Cao, et al., "Collaborative learning of graph generation, clustering and classification for brain networks diagnosis," *Computer Methods and Programs in Biomedicine*, vol. 219, 2022.

[11] M Simonovsky and N. Komodakis, "Dynamic edge-conditioned filters in convolutional neural networks on graphs," in *IEEE/CVF Conference on Computer Vision and Pattern Recognition (CVPR)*, 2017, pp. 3693–3702.

[12] P. Veličković, G Cucurull, A. Casanova, et al., "Graph Attention Networks," in *International Conference on Learning Representations (ICLR)*, 2018.

[13] A. Hammers, R. Allom, M. J. Koepp, et al., "Three-dimensional maximum probability atlas of the human brain, with particular reference to the temporal lobe," *Human Brain Mapping*, vol. 19, pp. 224–247, 2003.

[14] P.A. Yushkevich, Y. Gao, and G. Gerig, "ITK-SNAP: An interactive tool for semi-automatic segmentation of multi-modality biomedical images," in *38th Annual International Conference of the IEEE Engineering in Medicine and Biology Society (EMBC)*, 2016, pp. 3342–3345.

[15] Surveillance of Cerebral Palsy in Europe, "Surveillance of cerebral palsy in Europe: a collaboration of cerebral palsy surveys and registers," *Developmental Medicine and Child Neurology*, vol. 42, pp. 816–824, 2000.

[16] M. Fey and J.E. Lenssen, "Fast Graph Representation Learning with PyTorch Geometric," in *ICLR 2019 Workshop on Representation Learning on Graphs and Manifolds*, 2019.

[17] K.H. Brodersen, C.S. Ong, K.E. Stephan, and J.M. Buhmann, "The Balanced Accuracy and Its Posterior Distribution," in *20th International Conference on Pattern Recognition*, 2010, pp. 3121–3124.

[18] N. Hollmann, S. Müller, K. Eggensperger, and F. Hutter, "TabPFN: A Transformer That Solves Small Tabular Classification Problems in a Second," 2022.